Vacancy Dynamics and Reorganization on Bromine-Etched Si(100)-(2 × 1) Surfaces

Cari F. Herrmann and John J. Boland

Venable and Kenan Laboratories, Department of Chemistry, University of North Carolina, Chapel Hill, North Carolina 27599-3290

(Received 12 March 2001; revised manuscript received 6 June 2001; published 27 August 2001)

Halogen etching of Si(100) surfaces has long been considered to involve the selective removal of atoms from an essentially static surface. Here we show that vacancy sites produced by etching are mobile at elevated temperature and rearrange to form features that were considered to be the direct products of etching. We demonstrate that the etch features observed at different temperatures are not due to different mechanisms. Rather, kinetic etch products formed at low temperatures are transformed into thermodynamically more stable features at higher temperatures.

DOI: 10.1103/PhysRevLett.87.115503 PACS numbers: 61.72.Ff, 68.37.Ef, 81.65.Cf

Although halogen etching [1] of silicon surfaces is a key step in semiconductor processing, the mechanism of chemical etching is poorly understood. Figure 1(a) is a high-resolution empty-state scanning tunneling microscope (STM) image chosen to illustrate the types of vacancy and regrowth features typically found on a low temperature Br_2 etched Si(100) surface. Figure 1 also shows the currently accepted etch mechanism in which dimers on the Si(100) surface undergo a monobromide-dibromide isomerization that generates an adsorbed $SiBr_2$ species and a bare Si atom [2]. Under etching conditions, the Si atom escapes onto the terrace, leaving behind a single-atom vacancy (labeled SV in Fig. 1) and a dibromide species [3]. The Si atoms on the terrace nucleate to form regrowth islands (RI). In the final step, the dibromide species desorbs, producing a dimer vacancy (DV). Etching continues by successive removal of neighboring dimers, a process that ultimately produces strings of DVs that run parallel to the dimer row direction [4]. At higher temperatures, a new etching pathway emerges and results in the formation of alternating strings of SVs separated by rows of dimers, yielding a local 3×1 etch pattern [5].

A key aspect of the current model is that etching occurs on an essentially static surface, such that the final morphology reflects difference in the local rates of defect nucleation and the rates of defect propagation both along and perpendicular to the dimer row directions [4]. Implicit within this model is that the defects produced by chemical etching are immobile under etching conditions, so that their diffusional dynamics do not contribute to the morphology of the etched surface. Here, in this Letter, we address these issues by studying in real time the dynamics of etch-induced defects using a variable temperature scanning tunneling microscope (VT-STM). Specifically, we prepared surfaces with populations of SV and DV defects and recorded the vacancy dynamics as a function of temperature. Our study reveals that SVs and DVs, which are the immediate products of chemical etching, are both mobile even at temperatures where the etch rate is quite modest. Here we focus on SV dynamics; DV dynamics are discussed elsewhere [6]. SVs exhibit both intradimer and interdimer motion. SV motion results in the nucleation and growth of organized vacancy structures with a local 3×1 periodicity, structures that are similar to those reported on high temperature etched Si(100) surfaces. After the supply of SVs is depleted, the 3×1 structures continue to grow by the rearrangement of DV strings that preferentially nucleate nearby. These results demonstrate that vacancy diffusion occurs and has an important role in determining the morphology of etched surfaces.

Experimentally, samples were prepared by annealing 0.3–1.0 Ω cm phosphorous-doped Si(100) substrates to 1400 K to remove the native oxide. The clean surface was then annealed and exposed to Br_2 from an electrochemical cell [7]. The substrate temperature and bromine dose were used to control the type of etch vacancies (SV or DV) on the final surface. SVs are preferentially formed at lower etch temperatures, whereas DVs are dominant at higher preparation temperatures. SV surfaces were prepared by heating to 600 K in the presence of a 5.4×10^4 μA s Br_2 dose or a dose of ~1000 langmuir. Under these exposure conditions, the surface is fully Br passivated. After preparation, the surface was cooled to room temperature, and subsequently heated in the STM stage while images (empty-state, −1.7 V tip bias) were recorded from 300 to 900 K. The surface was imaged for several hours at each temperature with typical scan rates of 100 nm per sec. These acquisition rates allowed us to record vacancy diffusion and surface transformations that were slow on this time scale.

Figure 1(b) is a high-resolution empty-state STM image of the two vacancy types that occur on the Si(100) surface after Br_2 exposure. Note that under these bias conditions, the dark node in the STM image is located between the two atoms of the Si dimers. Dimer vacancies (labeled DV), where both Si dimer atoms are missing, appear as dark features spanning the full width of the dimer row. The STM intensity within DV sites is due to rebonding of the second-layer Si atoms (see schematic in Fig. 1). Single Si-atom vacancies (labeled SV) are imaged as small dark features half the width of the dimer row. To confirm that SVs are indeed single Si-atom vacancies rather

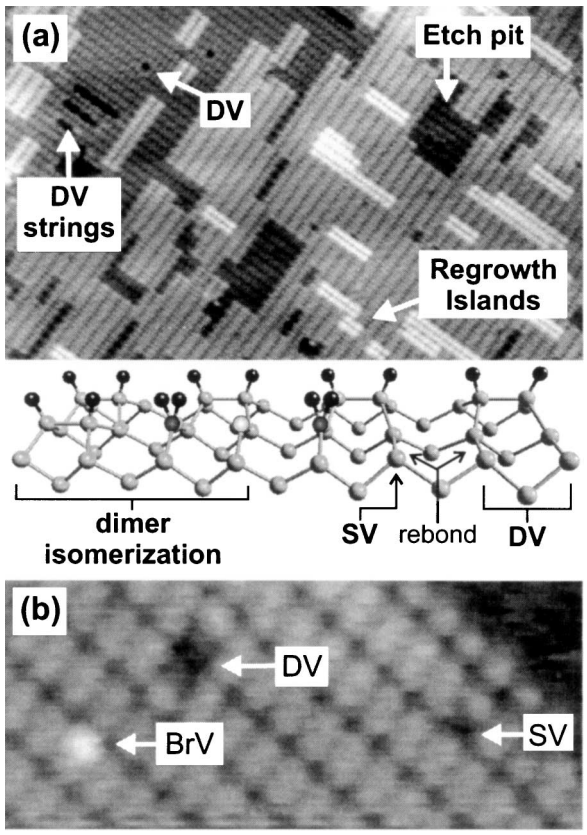

FIG. 1. (a) An STM image (22×44 nm^2, -1.7 V tip bias) of the bromine-passivated Si(100) surface after a 750 K etch that shows the characteristic features found after low temperature chemical etching. The surface contains DVs, DV strings, and RIs. The isomerization mechanism is shown schematically in the model from left to right. Isomerization produces a dibromide species (represented in the schematic by a darker Si atom) and a bare Si atom (represented by the lighter Si atom). Loss of the bare atom to the terrace produces an SV. Subsequent desorption of the dibromide species produces a DV. The second layer rebonds at SV and DV sites are also shown. (b) A high-resolution STM image (5×11 nm^2) illustrating three vacancy types: SV, DV, and Br adatom vacancy (BrV). Note that the dimer next to the SV site relaxes into the vacancy to reduce repulsive interactions between adjacent Br adatoms (see text).

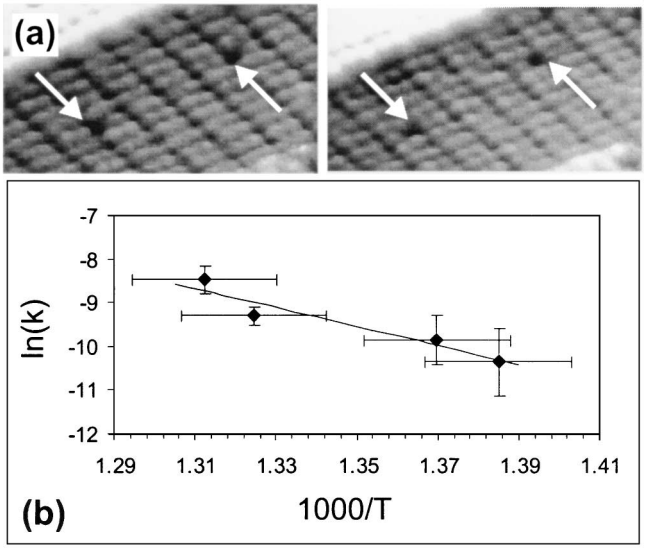

FIG. 2. (a) A series of STM images (4×7 nm^2) taken at 725 K depicting the single vacancy intradimer motion. The white arrows run down the center of the dimer row, clearly illustrating that the two single vacancies hop from one side of the dimer to the other. (b) Arrhenius plot for this intradimer motion reveals a hopping barrier of 1.9 ± 0.4 eV.

than Br-adatom vacancies we dosed a Si(100) surface with slightly less than one monolayer of Br_2 [see Fig. 1(b)]. In empty-state images, Br-adatom vacancies (labeled BrV) are 0.08 nm higher than the surrounding Br-passivated terrace due to the dangling bond at these sites and are thus clearly distinguishable from SVs.

SV populated surfaces were heated to increasingly higher temperatures to record the vacancy dynamics and surface reorganization using STM. Vacancy diffusion was not observed until about 700 K, at which point SVs undergo intradimer hopping during which the $SiBr_2$ species jumped back and forth in the vacancy site. Figure 2(a) shows two SVs exhibiting intradimer motion. Intradimer SV dynamics were recorded for various temperatures and the hopping rate was calculated for each. An Arrhenius plot of SV intradimer hopping is shown in Fig. 2(b). The data shown are restricted to a very limited temperature range over which intradimer SV motion occurred but not interdimer motion. The barrier observed for intradimer SV hopping is 1.9 ± 0.4 eV, the magnitude of the error bars reflect the restricted temperature range accessible for this analysis. This energy barrier is significantly higher than the 0.6 and 1.0 eV barriers for Si atom motion along and across dimer rows on the bare Si(100) surface [8], indicating the presence of halogen impedes but does not prevent motion [9].

At higher temperature, both interdimer and inter-row SV motion occur. These motions were not directly observed but inferred from the evolution of the surface structure. Figure 3(a) shows the SV population holds steady and then decays abruptly as the temperature increases. This decay is mirrored by the growth of organized vacancy structures we refer to as ladders [Fig. 3(b)], which are comprised of two SV strings separated by a single row of Si dimers [10]. This rapid, nonreversible SV coalescence into ladders makes it impossible to measure the energy barrier for interdimer and inter-row motion using the present method. Ladder formation conserves the number of surface Si and Br atoms. Two SVs and two $SiBr_2$ species are required for each rung of the ladder. The Br atoms from the $SiBr_2$ species are required to passivate the rebonded sites on the second layer Si atoms along the SV strings of the ladder (see Fig. 1). This transformation occurs over a very narrow temperature range ($\sim$770–790 K), after which no SVs remain on the surface [see Fig. 3(a)].

Although ladders randomly nucleate on the surface, their shapes are highly anisotropic with growth extending in the [011] dimer row direction. As the surface temperature

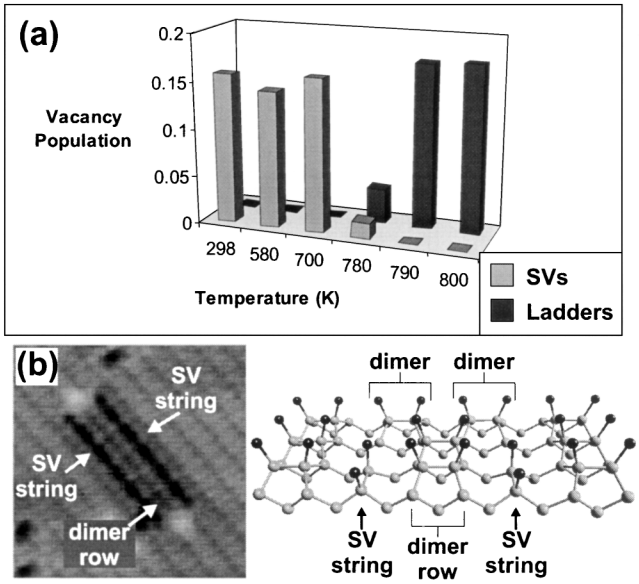

FIG. 3. (a) The decay of the SV population and growth of ladder population with temperature. (b) An empty-state STM image and a schematic of a ladder vacancy. The cross-sectional schematic shows that a ladder is composed of two rows of SVs separated by a monobromide dimer row with a shift in dimerization with respect to the neighboring 2×1 terrace. The schematic also illustrates the rebonds present at the second layer Si atoms.

is increased beyond 790 K, ladder vacancies continue to grow and eventually dominate the surface. Figure 4 shows a surface imaged at 800 K. We note that DV strings tend to form at the ends of ladders, a process that results in the formation of RIs [6]. Also at these high temperatures, the ladders themselves order side by side and extend in the perpendicular $[01\bar{1}]$ direction. The resulting SV string–Si dimer row–SV string pattern is identical to the local 3×1 pattern observed during etching (see schematic in Fig. 3). Thus not only does vacancy motion occur on Br-passivated surfaces, but it results in the formation etchlike features previously reported in the literature.

Figures 3(a) and 4 indicate that ladder growth continues even after the original SV population has been depleted. Additional vacancies are required for continued growth. Figure 5 shows two consecutive images recorded at 800 K, which demonstrates that ladder growth occurs by the formation and rearrangement of DVs or DV strings at the ends of ladder. The DV string at one end of the ladder in Fig. 5(a) rearranges with dimers in the adjacent row to produce SV-dimer-SV units in Fig. 5(b). This rearrangement conserves the number of surface Si and Br atoms and, in this case, extends the ladder by two rungs. We observe that this type of vacancy formation and rearrangement occurs preferentially at sites adjacent to existing ladders. These observations are consistent with recent calculations that indicate the presence of a strain-induced enhancement in the rate of dimer isomerization at sites next to existing defects [11]. We note that in the present case, dimer bonding

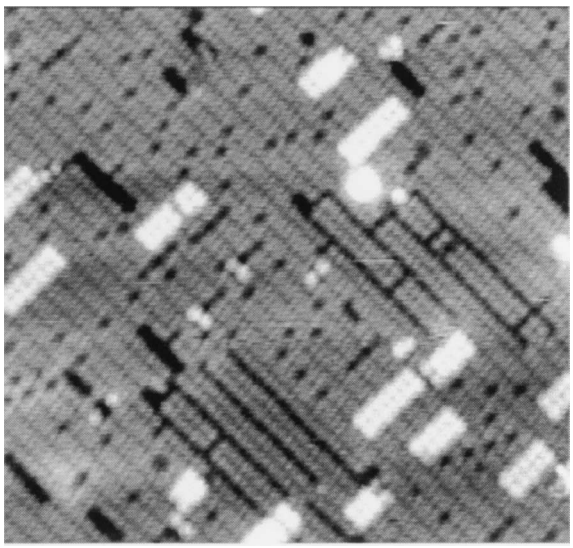

FIG. 4. A 20×21 nm^2 STM image recorded at 800 K, but on a different sample than that used in Fig. 3, illustrating that extensive ladder growth is accompanied by island regrowth after the initial SV population is consumed. For continued ladder growth, DVs are formed at the ends of ladders and extend the ladder structure. RI growth accompanies the DV formation.

within ladders is shifted with respect to that of the surrounding 2×1 surface (see schematic in Fig. 3). The enhanced brightness at the end boundary between ladders and these 2×1 regions is likely the result of the strain field introduced by the shift in dimerization [see Fig. 3(b)]. This dimer shift increases the tensile stress in the dimer bonds at the end boundary, and may promote dimer rearrangement.

The observation that ladder growth involves the rearrangement of DVs into SV-dimer-SV structures strongly suggests that the ladder or 3×1 structure is energetically preferred. We propose that the driving force for this reorganization is the steric repulsions that exist between

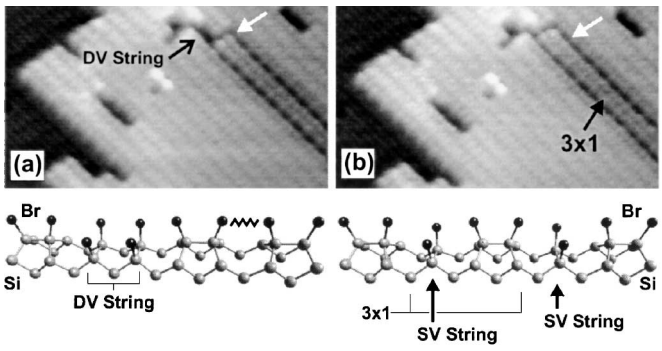

FIG. 5. A series of STM images (-1.7 V tip bias, 9×16 nm^2) recorded at 800 K that shows the growth of a ladder in (a) via the rearrangement of an adjacent DV string, (b). The white arrow marks the same position in each image and, in this case, the ladder is extended by two rungs. The schematics illustrate this rearrangement and show the reduction in repulsive interactions (represented by the zigzag line) between a surface containing a DV string and a 3×1 ladder structure.

Br atoms on adjacent dimers on adjacent rows of the Br-passivated Si(100)-(2 × 1) surface [12]. A comparison of the schematics in Fig. 5 shows that this rearrangement decreases the number of steric interactions. There are three key pieces of data that support this hypothesis. First, the 3 × 1 pattern is observed only when etching involves larger halogens (i.e., with Br_2 but not with Cl_2). Bromine adsorption on Si(100) is known to result in the formation of a repulsively stabilized $c(4 \times 2)$ structure in which bromine atoms avoid occupying adjacent dimers in adjacent rows [13]. Finally, a recent calculation has shown the Br-passivated 3 × 1 structure is lower in energy than the 2 × 1 surface due to reduced steric interactions [14]. Accordingly, a Br-etched surface containing DV strings will reorganize to form a 3 × 1 pattern of SV strings. Random DV string structures observed after low temperature etching are kinetics etch products of the original 2 × 1 surface that are slow to transform to the thermodynamically favored 3 × 1 structure.

Although ladders are identical in structure to the 3 × 1 etch patterns previously reported, there are notable differences in the formation kinetics. The 3 × 1 patterns occur predominantly under high temperature etch conditions (900 K and above). The ladders described here form at temperatures below 800 K by the coalescence of SVs. Clearly, the presence of SVs on the prepared surface facilitates the formation of 3 × 1 patterns at low temperatures. This does not occur when the surface is continuously exposed to Br_2 during low temperature (<900 K) etching. At temperatures below the lowest etching temperature, Br_2 reacts by inserting into the Si-Si dimer bond producing two adjacent $SiBr_2$ species [10]. Calculations indicate that this configuration is unstable, particularly at higher temperatures, and one $SiBr_2$ species can desorb with an extremely low (~1.4 eV) barrier [11] or react with an incident Br_2 molecule to form $SiBr_4$. However, the SV produced in this manner is stable since the barrier for desorption of the second $SiBr_2$ species is significantly higher (~2.9 eV in the case of chlorine [11]). The dimer insertion reaction becomes increasingly inefficient at higher temperatures [15], so that under real etching conditions the only route to SV formation is dimer isomerization, and this is quickly followed by DV formation. Consequently, there are few SVs available under typical etching conditions and higher temperatures are required to rearrange DVs into the thermodynamically preferred SV-dimer-SV structure characteristic of the 3 × 1 etch pattern.

In conclusion, vacancies are mobile under etching conditions and play an important role in determining the surface morphology. The 3 × 1 etch morphology is formed by the coalescence of SVs and extended by the rearrangement of DV strings that preferentially nucleate on the adjacent 2 × 1 terrace. These results demonstrate that the 3 × 1 structure is not formed by a special etching mechanism but the result of a transformation that eliminates kinetic etch products (DV strings) in favor of the thermodynamic products (SV-dimer-SV strings).

We acknowledge the National Science Foundation for financial support under Contract No. DMR9812416.

[1] H. F. Winters and J. W. Coburn, Surf. Sci. Rep. **14**, 161 (1992).
[2] M. Chander, D. A. Goetsch, C. M. Aldao, and J. H. Weaver, Phys. Rev. Lett. **74**, 2014 (1995); J. H. Weaver and C. M. Aldao, in *Morphological Organization in Epitaxial Growth and Removal,* edited by M. G. Lagally and Z. Zhang, World Scientific Series on Directions of Condensed Matter Physics Vol. 14 (World Scientific, Singapore, 1998).
[3] G. A. d Wijs, A. De Vita, and A. Selloni, Phys. Rev. Lett. **78**, 4877 (1997).
[4] F. J. Williams, C. M. Aldao, and J. H. Weaver, J. Vac. Sci. Technol. B **14**, 2519 (1996); C. M. Aldao and J. H. Weaver, Jpn. J. Appl. Phys. **36**, 2456 (1997).
[5] D. Rioux, R. J. Pechman, M. Chander, and J. H. Weaver, Phys. Rev. B **50**, 4430 (1994).
[6] C. F. Herrmann and J. J. Boland (to be published).
[7] R. D. Schnell, D. Rieger, A. Bogen, K. Wandelt, and W. Steinmann, Solid State Commun. **53**, 205 (1985).
[8] G. Brocks and P. J. Kelly, Phys. Rev. Lett. **66**, 1729 (1991).
[9] J. E. Vasek, Z. Y. Zhang, C. T. Salling, and M. G. Lagally, Phys. Rev. B **51**, 17 207 (1995).
[10] The darker appearance of the dimer row in the middle of the ladder is due to relaxation of the steric interactions between Si-Br bonds [6].
[11] G. A. d Wijs, A. De Vita, and A. Selloni, Phys. Rev. B **57**, 10 021 (1998).
[12] C. F. Herrmann and J. J. Boland, J. Phys. Chem. B **103**, 4207 (1999).
[13] C. F. Herrmann and J. J. Boland, Surf. Sci. **460**, 223 (2000).
[14] G. A. d Wijs and A. Selloni, Phys. Rev. B **64**, 041402 (2001).
[15] R. B. Jackman, R. J. Price, and J. S. Foord, Appl. Surf. Sci. **36**, 296 (1989); A. Szabo and T. Engel, J. Vac. Sci. Technol. A **12**, 648 (1994); M. C. Flowers, N. B. H. Jonathan, Y. Liu, and A. Morris, Surf. Sci. **343**, 133 (1995).